IEEE Access
Multidisciplinary | Rapid Review | Open Access Journal

Received April 10, 2020, accepted April 29, 2020, date of publication May 11, 2020, date of current version June 4, 2020.

Digital Object Identifier 10.1109/ACCESS.2020.2993598

A New Non-Smooth Simplified Model for DFIG in Electromechanical Transient Analysis

ANCHENG XUE[1], **(Member, IEEE), XIAOYU FU**[1], **DENGKE QIAO**[1], **RUIHUANG LIU**[1,2], **ZIZHE WANG**[1,3], **AND YU WU**[1,4]

[1]State Key Laboratory of Alternate Electrical Power System with Renewable Energy Source, North China Electric Power University, Beijing 102206, China
[2]Electric Power Science Research Institute of Jiangsu Electric Power Company, Ltd., Nanjing 210036, China
[3]State Grid Changzhou Power Supply Company of Jiangsu Electric Power Company, Ltd., Changzhou 213000, China
[4]State Grid Wuxi Power Supply Company of Jiangsu Electric Power Company, Ltd., Wuxi 214000, China

Corresponding author: Ancheng Xue (acxue@ncepu.edu.cn)

This work was supported by the National Key Research and Development Program under Grant 2017YFB0902000 and Grant 2017YFB0902004.

ABSTRACT The transient of the DFIG engages a lot of non-smooth elements such as switches of controllers and saturation of limiters, thus, the simplified non-smooth model of DFIG for electromechanical transient analysis is needed. This paper proposes a non-smooth simplified model of DFIG for electromechanical transient analysis, with the viewpoint of the transient response and energy accumulation. First, the general non-smooth dynamic behavior of DFIG during fault-on and post-fault periods are presented and the model is divided into four smooth stages. Then, the detailed model for the transient stage, according to without/with the trigger of the crowbar is presented. Furthermore, the simplified model of DFIG in the steady state is introduced according to without/with the trigger of the crowbar and saturation of limiters, determined by the stator voltage. Moreover, the transient model with/without the crowbar protection are simplified according to the principle of constant energy accumulation. Thus, the overall non-smooth simplified models of DFIG is obtained. Finally, the effectiveness of the proposed non-smooth simplified model is verified with the simulations.

INDEX TERMS DFIG, electromechanical transient analysis, energy accumulation, simplified mode.

I. INTRODUCTION

In recent years, WTG (wind power generator) represented by DFIG (doubly fed induction generator) has been connected to the power grid with a large scale [1]. The DFIG engages a different time scales than the conventional synchronous machine [2], which causes the serious transient stability problem of power system [3]–[13]. Thus, two basic questions about transient stability are concerned. The one is the transient stability of WTG itself [3], the other is the transient stability of power system due to the interconnection of WTG [4]–[13].

For the first problem, the detailed model for the WTG is used. It contains model for the wind turbine, the asynchronous generator and the control system. They were mainly modeled as multi-mass model [4], three-order model [5], and dimension-reduced model [6] respectively. The time domain simulation is the popular analysis method.

The associate editor coordinating the review of this manuscript and approving it for publication was Canbing Li.

However, for the second problem, some references use the detailed model. For example, Ref [7] considers the high-order general model of electromechanical transient of DFIG. Ref. [8] applied the detailed model of WTG to the rotor angle stability of system with thermal & wind power generation and AC/DC transmission through simulation.

Although the detailed model retains the dynamic of WTG, since the system interconnected with WTGs contains many equipment, but the full-scale model will cause the ''dimensionality disaster'', thus result in difficulty to analyze the mechanism of impact of wind farms on the transient behavior of the AC system. Therefore, some references use different simplified models of the DFIG [8]–[12]. For example, Ref. [9] models the asynchronous generator with a three-order model, and simplifies the electromechanical transient model of the rotor side converter and crowbar controller by transfer function method. Ref. [10], [11] considers the DFIG as a constant negative resistance to study the influence of WTG's interconnection on the power-angle curve and the transient stability of power system. Ref. [12]

models the DFIG as variable impedance, and analyzes the influence of its fault-on behavior on transient stability of system through extended equal area criterion (EEAC). Ref. [13] believes that the WTG has a characteristic of constant power after fault.

On the other hand, there are also work use the transient energy function (TEF) to analyze the transient stability of the WTG integrated power system [14]–[16]. For example, Ref. [14] proposes an unified method for transient stability assessment of system including WTGs based on corrected kinetic energy. Ref. [15] proposes the energy function of DFIG in the form of potential, reactive, and inertial energies. Ref. [16] considers the TEF of the system integrated with multiple DFIGs. Generally, the TEF is concerned with the energy of the WTG system in the post-fault period, but there is no analysis of the energy accumulation in the fault-on period.

The above works use a single simplified impedance or power source model, it is very convenient. However, since the actual WTG has different switched dynamic, such as trigger of crowbar corresponding to different faults, the single model may be different from the actual characters of WTG. Furthermore, with the large disturbance, a lot of limiter in the DFIG will be saturated, and this characteristic could be caught hardly by the single model. Thus, the transient of the DFIG should reflect the non-smooth elements such as switches of controllers and saturation of limiters, thus, the non-smooth model of DFIG for electromechanical transient analysis is needed.

In recognized the above problems, this paper proposed a non-smooth simplified model of DFIG for electromechanical transient analysis, with the viewpoint of the transient response and energy accumulation.

The contributions of this paper are as follows:

(1) The model of DFIG for the transient stage in fault-on and post-fault periods are simplified with the principle of constant energy accumulation.

(2) A non-smooth simplified model of DFIG for electromechanical transient analysis.

The remainders of the paper are organized as follows. In Section II, the general non-smooth dynamic behavior of DFIG during fault-on and post-fault period is presented and the model is divided into four smooth stages, i.e., the transient and the steady-state stage in fault-on and post-fault periods, respectively. In Section III, the detailed model for the transient stage, according to without/with the trigger of the crowbar is presented are proposed through formula deduction and analysis. In Section IV, the simplified steady-state model of DFIG is introduced according to without/with the trigger of the crowbar and saturation of limiters, determined by the stator voltage. In section V, the transient model with/ without the crowbar protection are reduced according to the principle of constant energy accumulation. In Section VI, the overall non-smooth simplified models of DFIG is presented. In Section VII, the error between the simplified model and the detailed model is analyzed by simulation, the effectiveness of simplification is verified. Finally, conclusions and discussions are presented in Section VIII.

II. GENERAL NON-SMOOTH MODEL FOR DFIG BASED ON SIMULATION

This section presents the general non-smooth dynamic behavior of DFIG based on simulation and shows that the model contains four smooth stages.

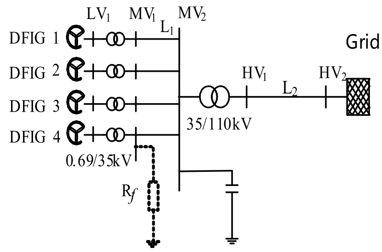

FIGURE 1. Schematic diagram of a regional wind farm.

Figure 1 shows the grid-connected system of a DFIG-based wind farm. The DFIGs are connected to the 0.69/35kV transformer at the bus MV_2 and then connected to the AC grid via a 35/110kV transformer. The operating parameters of the system can be referred to the appendix.

The dynamic of the above power system with respected to the fault can be divided into three periods, which are the pre-fault, fault-on and post-fault. When a fault occurs, the response of the crowbar of DFIG in the fault-on period can be divided into two cases according to the severity of fault, i.e., one is the crowbar triggered and the other is not, in the term of system, the fault-on system may switched to different smooth system according to the severity of fault.

The severity of the fault can be represented by the grounding resistance R_f of the three-phase fault at MV1. Here, two three-phase faults with different R_f resulting with the crowbar triggered/not triggered is considered. The fault occurs at MV1 at 1s, and then cleared at 1.5s.

Case 1: $R_f = 1\Omega$, the crowbar of DFIGs are triggered.

Case 2: $R_f = 3\Omega$, the crowbar of DFIGs are not triggered.

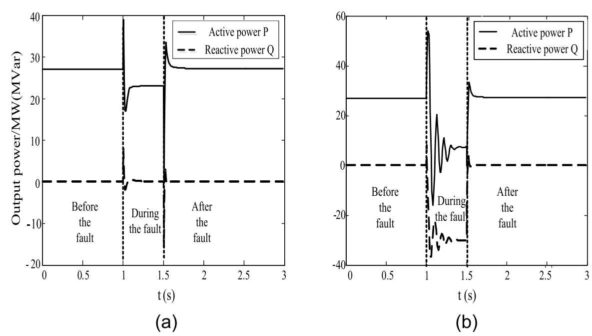

FIGURE 2. Output power of DFIG: (a) With the trigger of crowbar (b) without trigger of crowbar.

The output power of DFIG under the above two cases are shown in Fig. 2. The Fig.2 shows that no matter the crowbar is triggered or not, the output power of DFIG in fault-on and post-fault period go through a transient process before the steady state. According to the different output characteristics of the DFIG in the fault-on and post-fault periods, the dynamic of DFIG could be divide into four stages, i.e.,

(1) the transient stage in fault-on period
(2) the steady-state stage in fault-on period
(3) the transient stage in post-fault period
(4) the steady-state stage in post-fault period

For each stage, the DFIG is equivalent to different models according to whether the crowbar is triggered or not. They will be discussed in the following section.

Furthermore, with different R_f, the terminal voltage drops of the DFIG, which determining the saturation of limiter and trigger of the crowbar protection, is different. Thus, the non-smooth(switched) model is depended on the terminal voltage drop of DFIG.

III. DETAILED NON-SMOOTH MODEL OF DFIG AT TRANSIENT STAGE

This section presents the detail model of DFIG with/without the trigger of the crowbar.

A. WITHOUT THE TRIGGER OF THE CROWBAR

In the case of the crowbar is not triggered, the equivalent circuit of DFIG can be shown as in Fig. 3. Furthermore, its model can be described by the following equations.

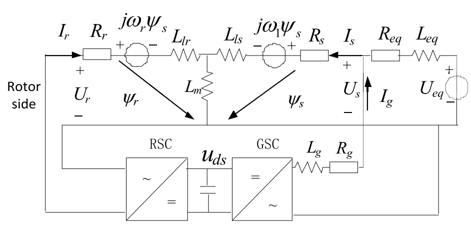

FIGURE 3. Equivalent circuit of DFIG.

Rotor shafting equation:

$$Mp\omega = P_t - P_e \tag{1}$$

Voltage equation:

$$\begin{cases} \tilde{U}_s = p\tilde{\psi}_s + R_s\tilde{I}_s + j\omega_1\tilde{\psi}_s \\ \tilde{U}_r = p\tilde{\psi}_r + R_r\tilde{I}_r + j\omega_s\tilde{\psi}_r \end{cases} \tag{2}$$

Flux linkage equation:

$$\begin{cases} \tilde{I}_s = \dfrac{L_r\tilde{\psi}_s - L_m\tilde{\psi}_r}{L_sL_r - L_m^2} \approx \dfrac{1}{L'}(\tilde{\psi}_s - \tilde{\psi}_r) \\ \tilde{I}_r = \dfrac{L_s\tilde{\psi}_r - L_m\tilde{\psi}_s}{L_sL_r - L_m^2} \approx \dfrac{1}{L'}(\tilde{\psi}_r - \tilde{\psi}_s) \end{cases} \tag{3}$$

Grid interface equation:

$$\tilde{U}_s = L_{eq}p(\tilde{I}_g - \tilde{I}_s) + R(\tilde{I}_g - \tilde{I}_s) + j\omega_1 L_{eq}(\tilde{I}_g - \tilde{I}_s) + \tilde{U}_{eq} \tag{4}$$

where $\tilde{\psi}_s(\tilde{\psi}_r)$ is the flux linkage of stator (rotor), $\tilde{I}_s$ $(\tilde{I}_r)$ is the current of stator (rotor), $\tilde{U}_s(\tilde{U}_r)$ is the voltage of stator (rotor); p is derivative operator; R_s (R_r) is the resistance of stator (rotor), L_s (L_r) is the self-inductance of stator (rotor) and L_m is the mutual-inductance between rotor and stator; ω_1 is the synchronous angular velocity, ω_r is the machine angular velocity and $\omega_s = \omega_1$-ω_r is the slip angular velocity; L_{eq} is the equivalent inductance; $\tilde{U}_{eq}$ is the equivalent voltage source of the network; $\tilde{I}_g$ is the current of the converter in grid side.

B. WITH THE TRIGGER OF THE CROWBAR

When crowbar is triggered, the rotor winding is shorted and the control system does not works, thus $\tilde{I}_g = 0$, $\tilde{U}_r = 0$ in (4), in this case, the DFIG is equivalent to a cage induction generator in this condition. What's more, according to Ref. [20], if there is a fault outside the wind farm or a fault with large grounding resistance inside the wind farm, the transient process in stator can be ignored, i.e., $p\tilde{\psi}_s = 0$ in (2). Meanwhile, it can be known from Ref. [18] that, the transient process of the grid connected to stator can be ignored generally when the stator transient process is neglected, i.e., $p(-\tilde{I}_s + \tilde{I}_g) = 0$ in (4). Then, the detailed model under this condition can be described by following equations.

Rotor shafting equation:

$$Mp\omega = P_t - P_e \tag{5}$$

Voltage equation:

$$\begin{cases} \tilde{U}_s = R_s\tilde{I}_s + j\omega_1\tilde{\psi}_s \\ \tilde{U}_r = p\tilde{\psi}_r + R_r\tilde{I}_r + j\omega_s\tilde{\psi}_r \end{cases} \tag{6}$$

Flux linkage equation:

$$\begin{cases} \tilde{I}_s = \dfrac{L_r\tilde{\psi}_s - L_m\tilde{\psi}_r}{L_sL_r - L_m^2} \approx \dfrac{1}{L'}(\tilde{\psi}_s - \tilde{\psi}_r) \\ \tilde{I}_r = \dfrac{L_s\tilde{\psi}_r - L_m\tilde{\psi}_s}{L_sL_r - L_m^2} \approx \dfrac{1}{L'}(\tilde{\psi}_r - \tilde{\psi}_s) \end{cases} \tag{7}$$

Grid interface equation:

$$\tilde{U}_s = -R_{eq}\tilde{I}_s - j\omega_1 L_{eq}\tilde{I}_s + \tilde{U}_{eq} \tag{8}$$

The above analysis indicates that the order of the detailed fault-on models of DFIG is high. Furthermore, in the case of the crowbar is not triggered, it is closely related to the control system. Thus, the detailed model is not suitable for the analysis of the impact of the interconnection of large-scale wind power. Therefore, the simplification of the detailed models is necessary.

IV. SIMPLIFIED MODEL FOR STEADY-STATE STAGES

This section deduces the simplified model of DFIG in the steady state stage according to without/with the trigger of the crowbar and saturation of limiters, determined by the stator voltage.

A. NON-SMOOTH MODEL FOR STEADY-STATE STAGE IN FAULT-ON PERIOD

1) WITHOUT THE TRIGGER OF THE CROWBAR

As stated in ref. [19] the steady-state active power output of DFIG is determined by the steady-state voltage in the fault-on period, as shown in Fig. 4. when the DFIG stator voltage satisfies $U_s > U_2$, then the crowbar is not triggered, and the steady-state reactive power output keeps zero, but the active power output have two different models according to stator voltage.

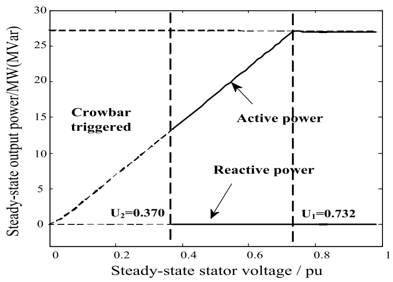

FIGURE 4. Active Power Output of DFIG without crowbar.

If the DFIG stator voltage satisfies $U_s > U_1$, the steady-state active power can maintain its output. In this case, the DFIG could be regarded as a constant active power source.

If the DFIG stator voltage satisfies $U_2 < U_s < U_1$, then, the steady-state active power is linear with the steady stator voltage, as the limiter of rotor current is saturated, the output equation is as follows,

$$P_{limit} = (1-s)\frac{L_m}{L_s} i_{rd}^{limit} U_s(t) \tag{9}$$

where L_m is the excitation reactance and L_s is the reactance of stator; $s = (\omega_1\text{-}\omega_r)/\omega_1$ is the slip ratio; i_{rd}^{limit} is the rotor limiting current; $U_s(t)$ is the instantaneous value of stator voltage.

In this case, the DFIG could be regarded as a constant active power current source.

2) WITH THE TRIGGER OF THE CROWBAR

The trigger of crowbar short the rotor winding, and control system will quit. Thus, the model of the DFIG is similar to a cage induction generator, as shown in Fig. 5.

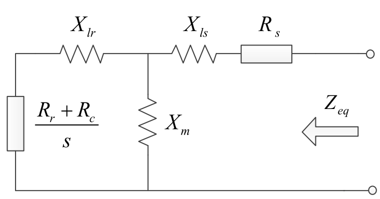

FIGURE 5. DFIG Steady state equivalent circuit in fault with crowbar.

where X_{ls} is the leakage reactance of stator, X_{lr} is the leakage reactance of rotor and X_m is the excitation reactance; R_c is the resistance of crowbar. If the excitation reactance is ignored, the equivalent impedance of DFIG is

$$Z_{eq} = \frac{R_r + R_c}{s} + R_s + j(X_{ls} + X_{lr}) \tag{10}$$

Furthermore, considering the speed of DFIG during the fault is approximately constant, i.e., $s = \text{const}$, then, the equivalent impedance of DFIG is approximately constant. Therefore, in this case, the DFIG can be simplified to a constant impedance.

B. MODEL OF STEADY-STAGE IN POST-FAULT PERIOD

In steady state after the fault, assuming the DFIG uses the maximum power point tracking control, then the DFIG active power output can be stated as follows,

$$P_{op} = K_w \omega_w^3 \tag{11}$$

where K_w is a constant related to wind turbine tip speed ratio, ω_w is wind turbine speed.

Equation (11) indicates that the steady-state active power output of DFIG is determined by wind turbine speed. Furthermore, as the inertia of wind turbine is large and the time constant of DFIG pitch angle control system is larger compared with the electromechanical transient time scale, so the steady-state active power output of DFIG is approximately constant. Thus, the model of DFIG for steady-state state in the post-fault model can be regarded as a constant active power source.

V. MODEL REDUCTION FOR TRANSIENT STAGE

This section presents the simplified model for the transient stage in the fault-on and post-fault periods based on the energy accumulation, according to without/with the trigger of the crowbar.

A. MODEL REDUCTION WITH THE TRIGGER OF THE CROWBAR

If crowbar is triggered, the detailed model of DFIG is described by (5)-(8). Furthermore, the transient current response of DFIG can be obtained as follows.

First, with (6)-(8), the algebraic relationship between stator flux linkage and rotor flux linkage can be obtained as follows,

$$(j\omega_1+\tau_a)\tilde{\psi}_s - \left(j\frac{L_{eq}}{L_{eq}+L'}\omega_1+\tau_a\right)\tilde{\psi}_r = \frac{L'}{L_{eq}+L'}\tilde{U}_{eq} \tag{12}$$

where $\tau_a = \left(R_s + R_{eq}\right)/\left(L' + L_{eq}\right)$.

For the (6), (7), (12), and reserved the stator flux linkage $\tilde{\psi}_s$, the following equation holds

$$p\tilde{\psi}_s + \frac{j\left(\tau_a\omega_s - \tau_2\omega_1 L_{eq}/(L_{eq}+L') + \tau_2\omega_1\right) - \omega_1\omega_s}{\tau_a + j\omega_1}\tilde{\psi}_s = \tilde{s} \tag{13}$$

where

$$\tau_1 = \left(R_s + R_{eq} - L_{eq}R_r/L'\right)/\left(L' + L_{eq}\right), \quad \tau_2 = R_r/L'$$
$$\tilde{s} = \frac{\tau_2 + j\omega_s}{\tau_a + j\omega_1}\frac{L'}{L' + L_{eq}}\tilde{U}_{eq} \tag{14}$$

For (13), as the constant τ_a, τ_b, τ_1, τ_2 are far less than ω_1 and ω_r (as shown in Table 7 of Appendix), then the following approximation can be obtained.

$$\tilde{\psi}_{s\_all}^{dq} = \tilde{\psi}_{sf}^{dq} + \tilde{\psi}_{sp}^{dq} = C_1^* e^{\tilde{\xi}t} + e^{\tilde{\xi}t}\int_0^t \tilde{s}e^{-\tilde{\xi}\lambda}d\lambda$$
$$\approx \frac{R_r/s + jX'}{R_r/s + j\left(X' + X_{eq}\right)}\frac{\tilde{U}_{eq}}{j\omega_1}\left(1 - e^{\tilde{\xi}t}\right) + C_1^* e^{\tilde{\xi}t} \quad (15)$$

where

$$\tilde{\xi} = -\tau_b\frac{\omega_1^2}{\tau_a^2 + \omega_1^2} - j(\omega_s + \frac{\tau_b}{\tau_a/\omega_1 + \omega_1/\tau_a}) = -\tau_b^* - j\omega_s^* \quad (16)$$

where τ_a^* is the reciprocal of flux decay time constant; ω_s^* is the rotation frequency; $\tilde{\psi}_{sf}^{dq} = C_1^* e^{\xi t}$ is the free response of stator flux linkage; C_1^* is an undetermined coefficient relating to initial values, $\tilde{\psi}_{sp}^{dq} = e^{\xi t}\int_0^t \tilde{s}e^{-\xi\lambda}d\lambda$ is the forced response of stator flux linkage.

For rotor flux linkage, the similar equation can be obtained as follows,

$$\tilde{\psi}_{r\_all}^{dq} \approx \frac{R_r/s}{R_r/s + j\left(X' + X_{eq}\right)}\frac{\tilde{U}_{eq}}{j\omega_1}\left(1 - e^{\tilde{\xi}t}\right) + C_2^* e^{\tilde{\xi}t} \quad (17)$$

Considering $\tilde{\psi}_r^{dq}\Big|_{t=0} = \psi_r(0)()$, then $C_2^* = \psi_r(0)$. Furthermore, with the relationship between (12) and (15), then at t =0, the following equation stands.

$$\tilde{C}_1^* \approx \frac{L_{eq}}{L' + L_{eq}}\tilde{\psi}_r(0) + \frac{L'}{L' + L_{eq}}\frac{U_{eq}}{j\omega_1} \quad (18)$$

Finally, with the flux linkage (7), the stator current in d-q frame can be obtained as follows

$$\tilde{I}_s^{dq} \approx \left[\frac{1}{X'+X_{eq}}\left(\frac{U_r(0^-)}{s} - U_{eq}\right) - \frac{\tilde{U}_{eq}}{R_r/s + j\left(X'+X_{eq}\right)}\right] \times e^{\tilde{\xi}t} + \frac{\tilde{U}_{eq}}{R_r/s+j\left(X'+X_{eq}\right)} \quad (19)$$

Equation (19) indicates that the stator current consists of two parts, one is the transient component of speed frequency which decay with time constant T_b, the other is the steady-state component of power frequency.

Among them, the steady-state power frequency component is equivalent to the induction generator model as shown in Fig. 7 in the case of the excitation reactance X_m and stator resistance R_s are ignored. This verifies that when the crowbar is triggered, the model of DFIG in steady-state can be regarded as an induction generator. Moreover, it can be simplified as a constant impedance.

For the transient decaying component, its frequency is slip frequency both in dq frame and xy frame, so the power corresponding to this component is decaying during the fault. On the other hand, it is the energy exchange between DFIG and large power system and it contributes little to energy accumulation. Thus, this component can be ignored in electromechanical transient analysis, according to the principle that unchanging the energy accumulation in the fault process.

Thus, if the DFIG stator voltage satisfies $U_S < U_2$, the constant impedance model for DFIG can be used in the electromechanical transient analysis.

B. MODEL REDUCTION WITHOUT THE TRIGGER OF THE CROWBAR

In the electromechanical transient stability analysis, the energy accumulation caused by the mismatch of mechanical power and electromagnetic power of the DFIG is the primary concern. Thus, this subsection simplifies the model from the perspective of output characteristic with the principle of the constant energy accumulation.

If crowbar is not triggered, then the $\tilde{U}_r$ and $\tilde{I}_g$ of the detailed model (1-4) in transient stage are determined by control system. Moreover, the control system is very complicated with several PI loops and limiters and switching dynamics. Therefore, it is difficult to analytically give out the detailed model. Here, the model is reduced with the energy accumulation.

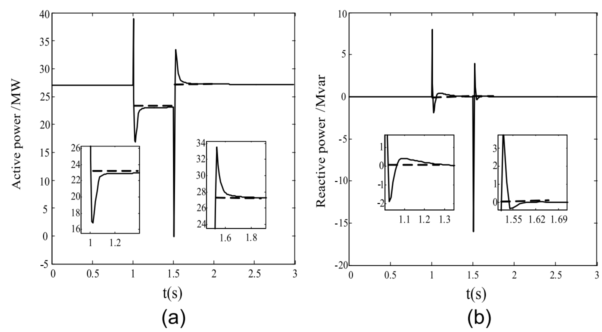

FIGURE 6. power Output under three-phase grounding fault by 3Ω resistance at MV_1. (a) Active Power Output (b) reactive power Output.

The output of DFIG can be obtained without the crowbar, as shown in Fig. 6. It indicates that the output in the transient stage for fault-on and post-fault period engaging a reverse transient process. The active output in the transient stage in fault-on period (1.0-1.2s in the example) is lower than the steady-state value and reversed in the post-fault transient process(1.5-1.7s in the example), so there is complementarity between the transient stage in fault-on and post-fault period.

Thus, the total energy accumulation produced by the two transient processes may be similar to the energy accumulation produced by the steady-state value (black dashed line). Thus, the transient model can be replaced by the steady-state model in the electromechanical transient analysis. i.e., when $U_S > U_1$, the model in the transient stage can be regarded as a constant power source, and when $U_2 < U_S < U_1$, the model in the transient stage can be regarded as a constant active current source.

VI. THE NON-SMOOTH SIMPLIFIED MODEL FOR DFIG

This section presents the overall non-smooth simplified models of DFIG. In general, the non-smooth simplified models at different stages can be obtained, as shown in Table 1.

TABLE 1. Non-smooth simplified model for DFIG at different stages.

DFIG stator voltage	Simplified model in fault-on period
$U_s>U_1$	Constant power source
$U_2<U_s<U_1$	Constant active power current source
$U_s<U_2$	Constant impedance

In detail, the proposed non-smooth simplified model for electromechanical transient analysis, is as follows.

For the fault-on period, the model is switched according to the DFIG stator voltage. if the crowbar and the current limit are not activated ($U_s > U_1$), the model can be the constant power source. If the crowbar is not triggered but the current limit is saturated ($U_2 < U_s < U_1$), the simplified fault-on model of DFIG can be the constant active current source. If the crowbar is triggered ($U_s < U_2$), the simplified fault-on model of DFIG can be the constant impedance.

For the DFIG in the post-fault, the simplified fault-on model of DFIG can be a constant power source.

VII. VERIFICATION FOR THE PROPOSED MODEL WITH SIMULATION

In this section, the proposed non-smooth is verified with the simulations in DIgSILENT, the system is shown in Fig.1.

A. VERIFICATION OF THE SIMPLIFIED TRANSIENT MODEL WITH CROWBAR TRIGGERED

In the simulation, a three-phase fault with 1Ω grounding resistance occurs at 1.0s at MV_1, and cleared at 1.5s. In this case, the crowbar is triggered. The equivalent fault-on impedance of the DFIG can be obtained as shown in Fig.7.

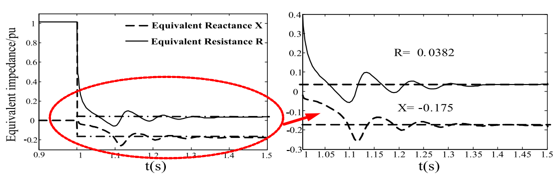

FIGURE 7. Equivalent impedance DFIG in fault with the crowbar is triggered.

As shown in Fig.7, when the fault occurs at 1.0s, the equivalent resistance and reactance drop rapidly from the pre-fault steady-state value (1pu- 0pu.). Then, it damply oscillates near the fault-on steady-state value (0.0382pu-0.175pu.) at the slip frequency. The above transient process lasts about 300ms. After that, the equivalent impedance approaches the fault-on steady-state value and remains unchanged. The dynamic process is coincided with the result as the process analysis in section V.

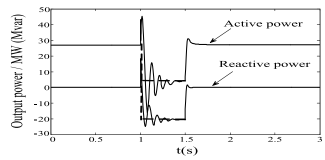

FIGURE 8. Power Output of DFIG under a three-phase fault with 1Ω grounding resistance at MV2.

Meanwhile, the active and reactive power output during the fault is shown in Fig.8. Both active power and reactive power oscillate near their steady-state value. According to model in section V, the transient energy accumulations may be replaced by the steady-state energy accumulations, as shown by the dashed line in Fig.7.

Furthermore, Table 2 shows that the energy accumulations produced by the high-order detailed simulation model and the constant impedance model in fault-on period(1s∼1.5s). The result confirms that the errors between the active/reactive power accumulation produced by constant impedance model and detailed transient model are blow 6%. Therefore, the high-order simulation model and the constant impedance model have a high degree of accuracy when the crowbar is triggered. Thus, the rationality of simplification is verified.

TABLE 2. Comparisons of energy accumulation with different models under crowbar trigger.

Power	Transient energy accumulation(kJ)		Error (%)
	Detailed model	Constant impedance model	
Active power	2.3577	2.2335	-5.27
Reactive power	-9.7037	-10.13	4.39

B. WITHOUT THE TRIGGER OF CROWBAR

In the simulation, a three-phase fault occurs at 1.0s at MV_1 in Fig.1, and cleared at 1.5s. The fault grounding resistance R_f is between 1.5Ω-5.0Ω. In this case, the crowbar will not be triggered. There are two cases.

Case 1: When R_f is between 1.5Ω-3.5Ω, the current limit is saturated and the steady-state model of DFIG is constant active current source (represented by C in Table. 3).

Case 2: When R_f is between 4.0Ω-5.0Ω, the current limit is not saturated and the steady-state model of DFIG is constant power source (represented by P in Table. 3).

Thus, simplified models are non-smooth and different according to different voltage drops. For the non-smooth simplified models, the comparison to detailed model, with the viewpoint of energy, can be obtained, as shown in Table 3. The energy accumulations are calculated in the fault-on transient period (1.0-1.2s) and post-fault transient period (1.5-1.7s).

The Table 3 shows that, when the crowbar is not triggered, the error between the total energy accumulations produced by the detailed model and simplified model is less than 2%. This range of error is acceptable when analyzing

TABLE 3. Comparisons of energy accumulation with deatailed/simplified model without crowbar.

U_s/pu	Simplified model	R_f/Ω	Energy Accumulation/kJ		Error (%)
			Detailed model	Simplified model	
0.7806	P	5.0	106.829	106.980	0.14
0.7556	P	4.5	106.580	106.980	0.35
0.7254	C	4.0	105.734	106.505	0.73
0.6878	C	3.5	102.807	103.445	0.62
0.6416	C	3.0	99.215	99.644	0.43
0.5841	C	2.5	94.767	94.683	-0.08
0.5118	C	2.0	89.205	88.418	-0.88
0.4204	C	1.5	82.281	80.700	-1.93

electromechanical transient characteristics. Thus, it is reasonable to using the proposed non-smooth simplified model to replace the detailed transient model in the electromechanical transient analysis when the crowbar is not triggered.

VIII. CONCLUSION AND DISCUSSIONS

This paper proposed a non-smooth simplified model of DFIG for electromechanical transient analysis, with the viewpoint of the transient response and energy accumulation. Specifically, the general non-smooth dynamic behavior of DFIG is divided into four smooth stage. In the four smooth stages, the simplified model of DFIG according to without/with the trigger of the crowbar and saturation of limiters, determined by the stator voltage, are introduced.

In detail, the proposed non-smooth simplified model are as follows. For the fault-on period, the model is switched according to the DFIG stator voltage. if the crowbar and the current limit is not activated the model can be the constant power source. If the crowbar is not triggered but the current limit is saturated, the simplified fault-on model of DFIG can be the constant active current source. If the crowbar is triggered, the simplified fault-on model of DFIG can be the constant impedance. For the DFIG in the post-fault, the simplified fault-on model of DFIG can be a constant power source.

The proposed non-smooth simplified model not only retains main features of DFIGs, but also could serve as a good foundation to under the transient stability of power system.

TABLE 4. The parameters of the DFIG.

Single capacity	1.5MW
Number	16*3+18*1
Stator leakage reactance	0.167pu
Rotor leakage reactance	0.1323pu
Excitation reactance	5.419pu
Stator resistance	0.0084pu
Rotor resistance	0.0083pu
Proportional gains K_{pq} and integral gains K_{ipq} of outer control loop	K_p=K_q=4, K_{ip}=K_{iq}=10
Proportional gains K_{dq} and integral gains K_{idq} of inner control loop	K_d=K_q=0.0496, K_{id}=K_{iq}=78.125

TABLE 5. The parameters of the transformers.

Box-type transformer	Capacity: 1600kVA Ratio of transformation: 0.69/35±2×2.5%kV U_k=6.5% I_0=0.6% P_0=1.69kW P_k=16.67kW
Main transformer	Capacity: 120MVA Ratio of transformation: 35/115±8×1.25%kV U_k=10.6% I_0=0.1% P_0=65.5kW P_k =359.2kW

TABLE 6. The parameters of the lines.

35kV Lines	Average length: 4.25km Impedance: 0.17+j0.365(Ω/km)
110kV Lines	Length: 17.55km Impedance: 0.07232+j0.396(Ω/km)
110kV Equivalent positive sequence	Minimum operational mode: 0.01511+j0.16978pu. Minimum operational mode: 0.01511+j0.16978pu.

TABLE 7. The values of τ_1 and τ_2 at different fault locations.

Fault Location	τ_1 (s^{-1})	τ_2 (s^{-1})
LV1	8.8173	8.7123
MV1	14.3704	8.7123
20%L1	14.5002	8.7123
40%L1	14.6298	8.7123
60%L1	14.7591	8.7123
80%L1	14.8881	8.7123
MV2	15.0168	8.7123
HV1	12.1266	8.7123
20%L2	13.0281	8.7123
40%L2	13.8861	8.7123
60%L2	14.7037	8.7123
80%L2	15.4838	8.7123
HV2	16.2289	8.7123

However, the reactive power and the protection in DFIG is not fully consider in this paper, as it mainly focuses on the active power and energy. Thus, it will become the future works.

APPENDIX

See Table 4–7.

ACKNOWLEDGEMENTS

The authors thank the anonymous reviewers for their helpful comments and suggestions.

REFERENCES

[1] T. Ackermann, *Wind Power in Power Systems*. Hoboken, NJ, USA: Wiley, 2005.

[2] P. Kundur, "Definition and classification of power system stability IEEE/CIGRE joint task force on stability terms and definitions," *IEEE Trans. Power Syst.*, vol. 19, no. 3, pp. 1387–1401, May 2004.

[3] J.-Y. Ruan, Z.-X. Lu, Y. Qiao, Y. Min, G.-H. Shao, X.-W. Xu, and K.-Y. Hou, "Transient stability of wind turbine adopting a generic model of DFIG and singularity-induced instability of generators/units with power–electronic interface," *IEEE Trans. Energy Convers.*, vol. 30, no. 3, pp. 1069–1080, Sep. 2015.

[4] H. Li, L. Han, and B. Zhao, "Effect of equivalent models of wind turbines on analysis results of transient stability for wind generator systems," *Proc. CSEE*, vol. 28, no. 17, pp. 105–111, 2008.
[5] S. K. Salman and A. L. J. Teo, "Windmill modelling consideration and factors influencing the stability of a grid-connected wind power-based embedded generator," *IEEE Trans. Power Syst.*, vol. 2, no. 18, pp. 793–802, Aug. 2003.
[6] J. Ouyang and X. Xiong, "Research on short-circuit current of doubly-fed induction generators under rotor excitation control," *Proc. CSEE*, vol. 34, no. 34, pp. 6083–6092, 2014.
[7] I. A. Hiskens, "Dynamics of type-3 wind turbine generator models," *IEEE Trans. Power Syst.*, vol. 27, no. 1, pp. 465–474, Dec. 2012.
[8] X. Guo, L. Zhao, and Y. Tang, "Study on angle transient stability for wind-thermal-bundled power transmitted by AC/DC system," *Proc. CSEE*, vol. 33, no. 22, pp. 19–25, 2013.
[9] P. Zi, X. Zhou, and F. Tian, "Electromechanical transient modelling of wind turbines based on doubly-fed induction generator," *Proc. CSEE*, vol. 35, no. 5, pp. 1106–1114, 2015.
[10] Y. Qiang, S. Huadong, T. Yong, Z. Bing, and G. Zhuoyuan, "Impact on angle stability of power system with doubly fed induction generators connected to grid," *Power Syst. Technol.*, vol. 37, no. 12, pp. 3399–3405, Dec. 2013.
[11] Q. Wang, A. Xue, and Y. Zheng, "Impact of DFIG-based wind power integration on the transient stability of power systems," *Power Syst. Technol.*, vol. 40, no. 03, pp. 875–881, 2016.
[12] X. Tian, W. Wang, Y. Chi, G. Li, H. Tang, and Y. Li, "Performances of DFIG-based wind turbines during system fault and its impacts on transient stability of power systems," *Autom. Electr. Power Syst.*, vol. 39, no. 10, pp. 16–21, May 2015.
[13] L. Tang, C. Shen, and X. Zhang, "Impact of large-scale wind power centralized integration on transient angle stability of power systems—-Part I: Theoretical foundation," *Proc. CSEE*, vol. 35, no. 15, pp. 3832–3842, 2015.
[14] M. Tajdinian, A. R. Seifi, and M. Allahbakhshi, "Transient stability of power grids comprising wind turbines: New formulation, implementation, and application in real-time assessment," *IEEE Syst. J.*, vol. 13, no. 1, pp. 894–905, Mar. 2019.
[15] R. Yousefian, R. Bhattarai, and S. Kamalasadan, "Transient stability enhancement of power grid with integrated wide area control of wind farms and synchronous generators," *IEEE Trans. Power Syst.*, vol. 32, no. 6, pp. 4818–4831, Nov. 2017.
[16] M. A. Chowdhury, N. Hosseinzadeh, H. R. Pota, and W. Shen, "Transient stability of power system integrated with doubly fed induction generator wind farms," *IET Renew. Power Gener.*, vol. 9, no. 2, pp. 184–194, Mar. 2015.
[17] X. Luo, J. Yi, and J. Zhang, "Research on influence of integrated wind plants on power angle stability based on output characteristic of DFIG," *Power Syst. Technol.*, vol. 39, no. 12, pp. 3401–3407, 2015.
[18] Y. Ni, S. Chen, and B. Zhang, *Dynamic Power System Analysis*. Beijing, China: Tsinghua Univ. Press, 2008.
[19] A. Xue, J. Geng, R. Liu, "Study on the impact of the limiter on the output characteristics of DFIG during a fault," *Electr. Power Automat. Equip.*, vol. 37, no. 10, pp. 29–33, 2017.
[20] A. Xue, R. Liu, and J. Geng, "Approximate analytical solution of transient free response of DFIG and its time scale analysis," *Trans. China Electrotechn. Soc.*, vol. 32, no. 24, pp. 220–229, Sep. 2017.

ANCHENG XUE (Member, IEEE) was born in Jiangsu, China, in 1979. He received the B.Sc. degree in applied mathematics and the Ph.D. degree in electrical engineering from Tsinghua University, Beijing, China, in 2001 and 2006, respectively. He held a postdoctoral position at the Institute of System Science, Chinese Academy of Sciences. He is currently a Professor with North China Electric Power University, where he joined, in March 2008. His research interests include the power system parameter identification driven by the model and data, dynamic stability analysis and security defense of the power grid, and secondary equipment reliability evaluation.

XIAOYU FU was born in Hunan, China, in 1996. He received the B.S. degree in electrical engineering from North China Electric Power University, where he is currently pursuing the master's degree. His research interest is analysis of safety and stability of new energy power systems.

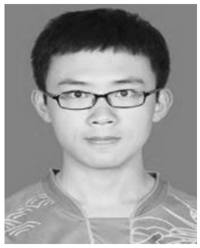

DENGKE QIAO was born in Hebei, China, in 1998. He received the B.S. degree in electrical engineering from North China Electric Power University, where he is currently pursuing the master's degree. His research interest is analysis of safety and stability of new energy power systems.

RUIHUANG LIU was born in Jiangsu, China, in 1992. He received the B.S. and master's degrees from North China Electric Power University. He is currently working with the Electric Power Science Research Institute of Jiangsu. His research interest is stability analysis and control of power systems.

ZIZHE WANG was born in Shandong, China, in 1995. He received the B.S. degree in electrical engineering from North China Electric Power University, where he is currently pursuing the master's degree. His research interest is analysis of wideband oscillation characteristics of PMSG.

YU WU was born in Shanxi, China, in 1994. He received the B.S. and master's degrees from North China Electric Power University. He is currently working with State Grid Jiangsu Wuxi Power Supply Company. His research interest is oscillation analysis and control of DFIG.